Indian Journal of Experimental Biology
Vol. 64, February 2026, pp. 127-140
DOI:10.56042/ijeb.v64i02.15900

Heterocyclic aromatic compounds from *Artemisia judaica* (L.) induced caspase-3 mediated apoptosis in metastatic breast cell lines

Fouzi S Aboud[1]*, Majed A Al-Shaeri[2], Ali T Zari[2], Ehab M M. Ali[3], Naif A Almalki[3], & Najat M Binothman[4]

[1]Department of Anatomy, Histology and Embryology, Faculty of Medicine, University of Tripoli, Tripoli, Libya

[2]Department of Biological Sciences, Faculty of Science, King Abdulaziz University, Jeddah, Saudi Arabia

[3]Department of Biochemistry, Faculty of Science, King Abdulaziz University, Jeddah, Saudi Arabia

[4]Department of Chemistry, Faculty of Sciences and Arts, King Abdulaziz University, Rabigh, Saudi Arabia

Received 28 January 2025; revised 01 December 2025

Chemoradiotherapeutic drugs remain a major clinical challenge for breast cancer patients due to their non-selective toxicity toward both malignant and healthy cells. The purpose of this study was to identify the aromatic organic compounds present in the ethanolic extract of *Artemisia judaica* (ArJ) and to evaluate their selective cytotoxic, oxidative-stress–mediated, and apoptosis-inducing effects against various breast cancer cell lines. In this study, several aromatic heterocycle compounds including benzamide, oxadiazine, benzofuran-carboxylic acid, and pyrimidine derivatives were identified in the ethanolic extract of ArJ using FT-IR and GC-MS spectral analysis. The cytotoxic and antiproliferative activities of the extract were assessed in normal human skin fibroblasts (HSF) and breast cancer cell lines (MCF-7, T47D, and MDA-MB-231) following 24 and 48 hours of treatment. ArJ extract exhibited minimal toxicity toward HSF cells (IC_{50} = 123.9 ± 3.86 µg/mL; selectivity index > 2), whereas a pronounced, time-dependent cytotoxic effect was observed in the metastatic MDA-MB-231 cells, with IC_{50} values of 35.62 ± 2.29 µg/mL, 16.93 ± 2.17 µg/mL, and 9.76 ± 2.03 µg/mL at 24, 48, and 72 hours, respectively. Treatment with ArJ significantly increased intracellular reactive oxygen species (ROS), disrupted mitochondrial membrane potential, and elevated caspase-3 activity, leading to cell-cycle arrest and apoptosis. In contrast, doxorubicin induced higher necrotic cell death and demonstrated greater toxicity toward normal cells. These findings suggest that the aromatic organic compounds present in ArJ exert selective and potent anticancer effects particularly against metastatic MDA-MB-231 cells through a ROS-mediated, mitochondrial caspase-dependent apoptotic pathway, highlighting their potential as safer alternatives to conventional chemotherapeutics.

Keywords: Apoptosis, Aromatics, Caspase-dependent mitochondrial pathway, Cytotoxicity, Spectroscopy analysis, Triple-negative breast carcinoma

Breast cancer (BC) accounts for nearly 30% of all female malignancies and remains the most diagnosed cancer among women worldwide[1]. According to the International Agency for Research on Cancer (IARC), an estimated 2.26 million new BC cases were reported in 2020, surpassing lung cancer by approximately 60,000 cases and representing 24.5% of all new cancers in women[2]. Most BCs are carcinomas and are classified into four major molecular subtypes based on invasiveness, pathological features, and hormonal receptor expression: luminal A (ER^+, $PR^{\pm}$, $HER2^-$), luminal B (ER^+, $PR^{\pm}$, $HER2^{\pm}$), HER2-enriched (ER^-, PR^-, $HER2^+$), and triple-negative breast cancer (TNBC) (ER^-, PR^-, $HER2^-$)[3].

Among these subtypes, TNBC accounts for 10–15% of cases and is associated with the poorest clinical prognosis, largely due to its lack of hormone receptors and the absence of targeted therapies[4]. Although estrogen receptor alpha (ERα) is absent in TNBC, some tumors retain estrogen responsiveness through alternative receptors such as estrogen receptor beta (ERβ) and the G protein-coupled estrogen receptor (GPER-1). Additionally, constitutively active estrogen-related receptors (ERRs) may further modulate estrogen-linked signaling pathways in TNBC[5].

Artemisia judaica L. (ArJ), a member of the family Asteraceae, is an aromatic medicinal herb rich in diverse phytochemicals, including phenylpropanoids, terpenoids, quinones, alkaloids, phenols, flavonoids, and various volatile compounds[6]. Previous studies have demonstrated its broad pharmacological activities, such as antioxidant, anti-inflammatory, anticancer, antidepressant, hepatoprotective and gastroprotective effects[7-9].

*Correspondence:
Phone: + 21891 5981973
E-mail: f.miftah@uot.edu.ly

Anticancer chemotherapy continues to pose major challenges for clinicians, despite advancements that have improved treatment efficacy and patient survival. Current strategies aimed at reducing chemotherapy-induced side effects remain inadequate. One of the most significant obstacles in cancer therapy is the ability to selectively eliminate tumor cells while sparing normal, healthy tissues. Cancer cells employ multiple mechanisms to evade or suppress programmed cell death pathways, enabling their survival and progression. Tumor eradication can occur through several forms of cell death, including apoptosis, necrosis, autophagy, and pyroptosis[10]. Among these, apoptosis plays a particularly central role and has been strongly linked to the pathophysiological processes underlying cancer development and resistance[11,12]. Emerging evidence shows that various natural products contain bioactive compounds capable of activating apoptotic signaling pathways[13]. These findings have encouraged extensive exploration of natural compounds as potential chemopreventive and chemotherapeutic agents, owing to their broad availability, lower toxicity and reduced likelihood of adverse effects.

Apoptosis is characterised by a highly regulated sequence of morphological events, including nuclear condensation, DNA fragmentation, plasma membrane blebbing, and the formation of apoptotic bodies that facilitate normal tissue homeostasis and embryonic development[14]. The intrinsic apoptotic pathway, which culminates in the activation of caspase-3, is essential for executing these changes. Disruptions or defects in this pathway can contribute to various pathological conditions, including cancer[15]. Consequently, many emerging therapeutic strategies aim to induce apoptosis in cancer cells through either intrinsic or extrinsic signaling mechanisms. These approaches target cellular survival pathways and the tumor microenvironment, seeking to suppress proliferation and promote programmed cell death[16].

In this study, we investigate organic compounds isolated from the ethanolic extract of *Artemisia judaica* leaves as potential anticancer agents against several BC cell lines. We hypothesise that these compounds induce apoptosis through activation of the intrinsic mitochondrial pathway, particularly via caspase-3 activation, with selective effects against the metastatic TNBC cell line MDA-MB-231.

Materials and Methods

Collection and identification of plant samples

Fresh leaves of ArJ were collected from Qitaf Radwa Farm, located in the Yanbu governorate at the centre of Radwa Mountain in the western region of Al-Madinah Al-Munawwara, KSA. Plant identification and authentication were performed by Dr. Faraj Abdullah Algamdi, Professor of Plant Taxonomy, Department of Biology, Faculty of Sciences, King Abdulaziz University, and a voucher specimen (ArJ18003) was deposited in the departmental herbarium.

Extraction of plant

A total of 20 g of finely powdered ArJ leaves were extracted using 200 mL of 80% ethanol (Merck®) in a Soxhlet apparatus for 24 hours. The crude extract was concentrated under reduced pressure using a rotary evaporator (Thermo-Fisher Scientific®) at 40°C, followed by lyophilization for 42 hours. The dried extract was stored at -20°C until further use.

Phytochemical screening

Functional groups present in the ethanolic extract were identified by Fourier-transform infrared (FT-IR) spectroscopy. A small quantity of the extract was placed on a sample holder, and spectra were recorded between 4000–500 cm^{-1}. Peaks were interpreted by comparison with previously reported spectra for similar phytochemicals[17,18]. Bioactive constituents were further characterised using gas chromatography–mass spectrometry (GC–MS) with a capillary column. Samples were injected in split mode at 300°C, with helium as the carrier gas at a flow rate of 1.61 mL/min (280°C). The GC temperature program involved a gradual increase of 10°C/min from 50°C to 300°C. The total run time was 32 minutes, with scans acquired across m/z 40–500. Compound identification was performed using the NIST 98 mass spectral library[19].

Cell culture and chemicals

Normal human skin fibroblasts (HSF) and breast cancer cell lines MCF-7, T47D, and MDA-MB-231 were obtained from the King Fahd Medical Research Centre (KFMRC), Jeddah, KSA. Cells were cultured in Dulbecco's Modified Eagle Medium (DMEM; HyClone®) supplemented with 10% fetal bovine serum, 100 U/mL penicillin G, and 100 µg/mL streptomycin at 37°C in a humidified incubator with

5% CO_2. Lyophilized ArJ extract was dissolved in dimethyl sulfoxide (DMSO; Sigma-Aldrich®) to obtain a stock concentration of 100 mg/mL. Doxorubicin (DOX; Swiss Parenterals Ltd®) stock solution (20 mg/mL) was freshly prepared by dissolving 10 mg of DOX powder in 500 µL of DMSO and used within 1 hour to minimize degradation. A working solution (50 µg/mL) was prepared by diluting 2.5 µL of the stock solution into 997.5 µL of DMEM. Serial 1:10 dilutions were subsequently prepared in 96-well plates to achieve the desired treatment concentrations.

Experimental design

HSF, MCF-7, T47D and MDA-MB-231 cells were seeded at 1 × 10^4 cells/well in 96-well plates containing 200 µL of medium. HSF cells were treated with DOX (3.125–50 µg/mL) or ArJ extract (6.25–100 µg/mL) for 24 hours to assess acute toxicity. BC cell lines were treated with the same concentration range of DOX and ArJ for 24 hours and 48 hours to determine cell viability. Mechanistic experiments including reactive oxygen species (ROS) generation, mitochondrial membrane potential (MMP) disruption, caspase-3 activity, and flow-cytometric analysis were performed exclusively on the MDA-MB-231 cell line because it exhibited the highest sensitivity to ArJ extract, as demonstrated by the lowest IC_{50} values at 24, 48, and 72 hours compared to MCF-7 and T47D cells. MDA-MB-231 also represents the most clinically aggressive TNBC phenotype, making it the most appropriate model for evaluating apoptosis-related mechanisms. For ROS, MMP, cell cycle and apoptosis assays, cells (5 × 10^5) were seeded in 6-well plates for 24 hours, then treated with IC_{50} concentrations of ArJ (30 µg/mL) or DOX (2 µg/mL) for 24 hours. For the caspase-3 assay, cells (8 × 10^3) were seeded in 96-well plates and treated with DOX (1.5, 3, and 6 µg/mL) or ArJ (25, 50, and 100 µg/mL).

MTT cell viability assay

Cell viability was assessed using the MTT assay according to Kamiloglu *et al*.[20]. Briefly, MTT (5 mg/mL) was dissolved in Dulbecco′s Phosphate Buffered Saline (DPBS, pH 7.4) and filtered through a 0.2 µm filter into a sterile, light-protected container prior to use. Experimental cells were seeded, cultured, and treated as described previously. At the end of the treatment periods (24, 48, and 72 hours), 10 µL of MTT solution (3-[4,5-dimethylthiazol-2-yl]-2, 5-diphenyltetrazolium bromide; Sigma-Aldrich®) was added to each well and incubated for 3 hours at 37°C. The resulting formazan crystals were dissolved in 100 µL of DMSO by gently rotating the plates for 10 minutes. Cell viability was quantified by measuring absorbance at 490 nm using a microplate reader. Three biological replicates were performed, each containing three technical replicates per treatment condition.

Selectivity index (SI) calculation

The selectivity index (SI) was calculated as:

$$SI = \frac{IC_{50}(\text{non-malignant cells})}{IC_{50}(\text{malignant cells})}$$

And SI range of 1.96–51.3 was considered significant for medicinal plant–derived compounds[21].

Microscopic examination

HSF cell morphology was examined after 24 hours of treatment using an inverted microscope. Morphological alterations in MCF-7, T47D, and MDA-MB-231 BC cells were assessed after 24 and 48 hours, and additional imaging of MDA-MB-231 cells was performed after 72 hours to evaluate time-dependent changes. Images were captured using a Leica 12.5-megapixel digital camera.

ROS assay

Intracellular ROS levels were quantified using CellROS Green (Invitrogen®). A total of 200 µL of MDA-MB-231 cell suspension was incubated with 2 µL of 50 mM CellROS Green. Samples were analyzed using the Amnis Flow Sight® cytometer, with Stream FlowSite software used to acquire and process data[22]. The ROS assay was performed with three technical replicates and two biological replicates to ensure measurement reliability and reproducibility.

MMP assay

MMP disruption was assessed using the JC-1 Staining Kit (Sigma-Aldrich®). A total of 200 µL of MDA-MB-231 cell suspension was incubated with 2 µl of 20 µM JC-1 dye (Invitrogen®, USA) at 37°C for 30 minutes. Following incubation, mitochondrial depolarization was evaluated by measuring blue fluorescence (JC-1 aggregates) using a BD FACSAria III flow cytometer[23]. MMP was performed using three biological replicates.

Caspase-3 activity assay

Caspase-3 activity was measured using the Caspase-Glo® 3 Assay (Promega®). MDA-MB-231 cells were treated for 4 hours, after which the Caspase-Glo reagent was added directly to each well without removing the culture medium. Samples were then incubated for 3 hours at room temperature, and caspase activity was quantified by recording the resulting luminescence. Caspase-3 activity assays were conducted using three biological replicates with three technical replicates per dose.

Cell cycle analysis

The BC MDA-MB-231 cells were harvested after 24 hours of treatment, fixed in 70% cold ethanol for 30 minutes at 4°C, and subsequently washed with PBS. The fixed cells were incubated with RNase A to remove RNA interference. Propidium iodide (PI; Sigma-Aldrich®) was then added, and samples were stained for 30 minutes at room temperature. DNA content was quantified using a BD FACSAria III flow cytometer to determine cell-cycle distribution[24]. Cell cycle analysis was conducted using three independent biological replicates.

Apoptosis assay

Apoptotic cell death was assessed using Annexin V-FITC/PI dual staining. After 24 hours of treatment, MDA-MB-231 cells were collected, washed with PBS, and centrifuged at 1500 rpm for 5 minutes. The cell pellets were resuspended in binding buffer, followed by the addition of Annexin V-FITC and propidium iodide (PI). Samples were incubated in the dark at room temperature, and fluorescence signals were analysed using a BD FACSAria III flow cytometer to quantify viable, early apoptotic, and late apoptotic cell populations[25]. Apoptosis assays were performed using three biological replicates.

Statistical analysis

Data are expressed as mean ± standard deviation from three independent experiments. Statistical differences between treated and untreated groups were analysed using one-way ANOVA, followed by Tukey's multiple comparison test (GraphPad Prism 8). A P-value < 0.05 was considered statistically significant.

Results

Isolation of phytochemical constituents

FT-IR analysis identified several major functional groups in the ethanolic extract of ArJ. A broad peak at 3310 cm^{-1} corresponded to O–H stretching of phenolic compounds, while a prominent peak at 1610 cm^{-1} indicated the presence of aromatic C=C and amine (N–H) groups. An additional peak at 1710 cm^{-1} was attributed to ester (C=O) stretching (Table 1, Fig. 1A).

Table 1 — FT-IR spectral peak characterisation of *A. judaica* L

Wave number (cm^{-1})	Intensity	Bond responsible
3380	2.93	ν:O-H (Phenolic, Alcohol)
2970	0.94	ν:C-H (Methyl & Methylene)
1710	1.77	ν:C=O (Ester)
1610	2.02	ν:C=C (Aromatic rings), N-H (Amine)
1420	1.11	δ:C-H (Saccharides)
1370	1.41	δ:C-H (Ester)
1230	0.98	ν:C-O (Ester, glycoside)
1050	1.50	ν:C-O (Alcohol, acid, Saccharides)

[ν: stretching; δ: bending]

GC–MS analysis revealed a total of 19 distinct compounds in the extract. Their retention times and relative peak area intensities are listed in Table 2. Most compounds eluted between 6.0 and 20.0 minutes, as shown in the chromatogram (Table 2, Fig. 1B).

Cell death analysis

Initial cytotoxicity screening using the MTT assay demonstrated that DOX markedly reduced the viability of normal HSF with an IC_{50} of 1.135 ± 0.35 µg/mL (Fig. 2A). In contrast, the ethanolic extract of ArJ exhibited minimal toxicity toward HSF cells, with an IC_{50} of 123.9 ± 3.86 µg/mL (Fig. 3A). In BC cells, DOX showed comparable potency, with an IC_{50} of 1.27 ± 0.12 µg/mL in MDA-MB-231 cells (Fig. 4A). ArJ extract, however, displayed selective antiproliferative activity across BC cell lines. In MCF-7 cells, the IC_{50} values were 78.22 ± 3.32 µg/mL and 65.07 ± 2.23 µg/mL after 24 and 48 hours of treatment, respectively (Fig. 5A). Similarly, T47D cells exhibited IC_{50} values of 98.7 ± 3.88 µg/mL and 77.43 ± 3.22 µg/mL for the same time points (Fig. 6A). The highest sensitivity was observed in the MDA-MB-231 TNBC cells, with IC_{50} values of 35.62 ± 2.29 µg/mL and 16.93 ± 2.17 µg/mL at 24 and 48 hours, respectively (Fig. 7A). Extended exposure of MDA-MB-231 cells to ArJ for 72 hours further reduced cell viability (IC_{50} = 9.76 ± 2.03 µg/mL), confirming a time-dependent cytotoxic effect (Table 3, Fig. 8A).

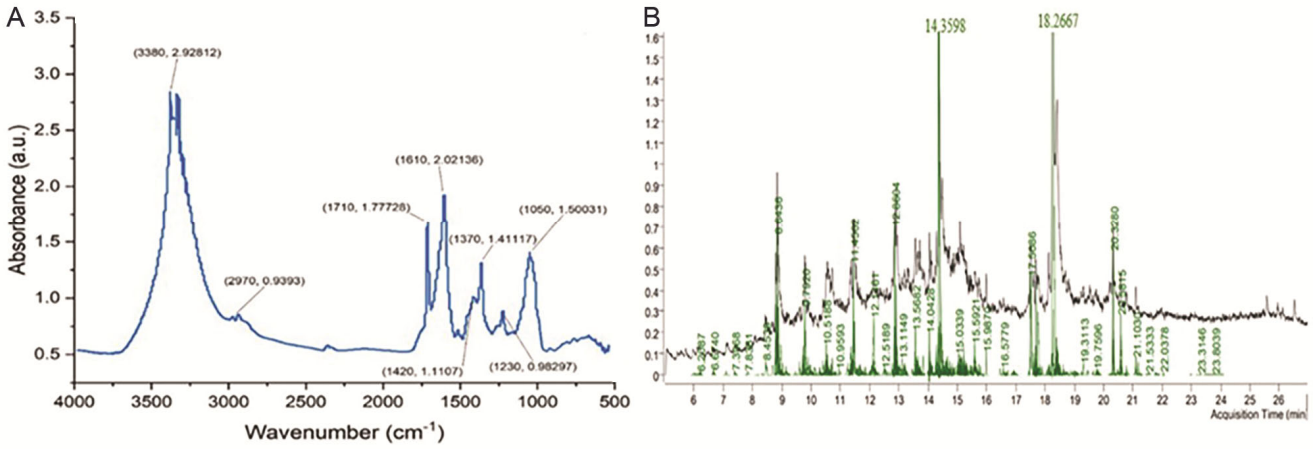

Fig. 1 — Spectroscopy analytical techniques showing: (A) FT-IR and (B) GC-MS spectral analysis identified the main bioactive compounds in *A. judaica* L.

Table 2 —GC-MS spectral analysis of *A. judaica* L

Peak	Retention Time	Compounds	Relative Peak Area Intensities
1	6.0187	Imidazolo-pyridine-6-carbonitrile	62.6
2	8.1953	5-(4-Bromobenzyl)-Oxoimidazolidine-1-carboxylic acid	57.9
3	8.6936	1,2-Benzenediol, O-(4-fluorobenzoyl)-O'-phenylacetyl	51.5
4	9.6401	4,6-Bis(4-ethoxybenzylthio)-5-nitropyrimidine	64.6
5	11.3577	3-Trifluoromethylbenzoic acid, 4-nitrophenyl ester	67.7
6	11.6097	Benzamide,3-benzimidazol-2-yl)-1,2,5-oxadiazol-	53.4
7	11.8533	3-Phenyl-6-triazolo-oxadiazin-4-one	55.0
8	14.3598	1H-1,2,3-Triazole-4-carboxylic acid-oxadiazol-3-yl	57.3
9	14.6274	5-Nitrothiophene-2-carboxaldehyde picolinoylhydrazone	50.2
10	15.2212	Acetic acid, (dodecahydro-7-hydroxy-tetramethyl-phenan threnylidene)-,2-(dimethyl amino)-ethyl	61.4
11	15.7238	Benzoic acid, 4-(diphenylphosphinoxido) methyl-, ethyl ester	54.5
12	16.6706	Benzamide, 3-methyl-N-(2-bromophenyl)-	52.5
13	17.7274	1,3-Benzenediol, O, O'-di(cyclopropanecarbonyl)-	55.3
14	17.7515	2-Benzofurancarboxylic acid-trimethyl-1,2-dioxetan-3-yl	55.9
15	18.4049	Tetrahydropyrimidine-5-carboximidamide	52.5
16	18.4749	2-Amino-4,6-diphenylpyrimidine	63.0
17	18.4832	3a,6-Epoxy-3aH-isoindole, a-hexahydro-6-methyl-2-phenyl-	52.5
18	18.4913	4-Methoxy-N-methylphenylethylamine, pentafluorpropionyl	51.0
19	20.4748	2-Trifluoromethylbenzoic acid, 2-bromo-4-fluorophenyl ester	50.6

SI analysis

The SI values were calculated to evaluate the ability of ArJ extract to preferentially target cancer cells over normal HSF cells, as presented in Table 4. At 24 hours, ArJ exhibited SI values of 1.58 for MCF-7, 1.25 for T47D, and 3.48 for MDA-MB-231. After 48 hours, the SI values increased slightly for the hormone-dependent cell lines (1.90 for MCF-7 and 1.60 for T47D) and showed a substantial rise for the metastatic MDA-MB-231 cells (7.31). These values approach or exceed the recommended selectivity range of 1.96–51.3 for plant-derived compounds, particularly in the highly aggressive MDA-MB-231 line, indicating a strong preferential cytotoxicity toward TNBC cells as exposure time increases. In contrast, DOX demonstrated an SI < 1 (not selective), reflecting higher toxicity toward normal cells. Overall, the SI profile confirms that ArJ extract possesses favourable and time-dependent selectivity, with the most pronounced therapeutic window observed in metastatic TNBC cells.

Cell morphology analysis

Morphological examination showed that DOX-treated HSF cells displayed significant structural

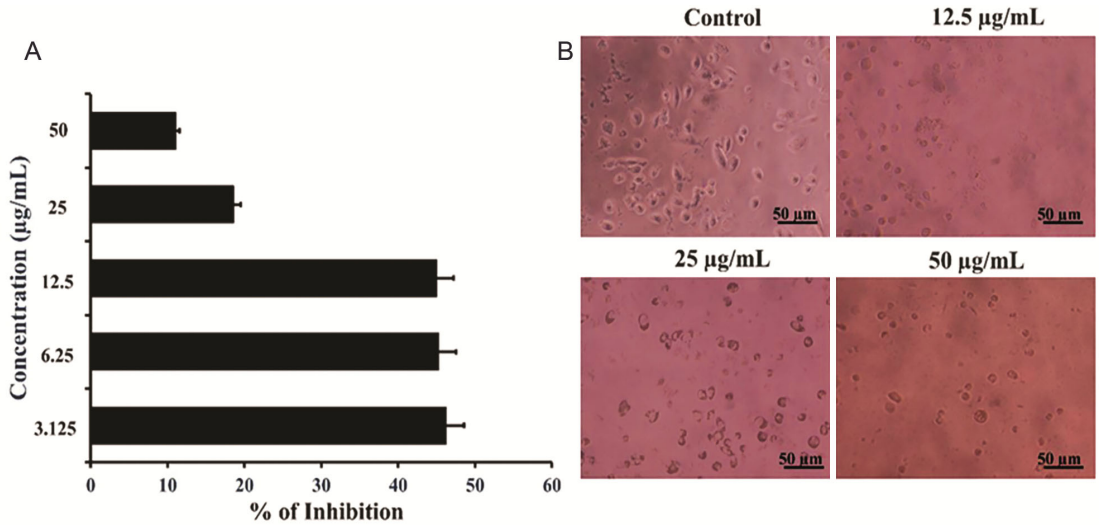

Fig. 2 — Cell death analysis of DOX-treated normal HSF cells.MTT assay showing: (A) Cell viability and (B) Morphological changes of treated cells at various concentrations for 24 h of treatment. Images were acquired using an inverted microscope (LABOMED®) at 20× magnification.

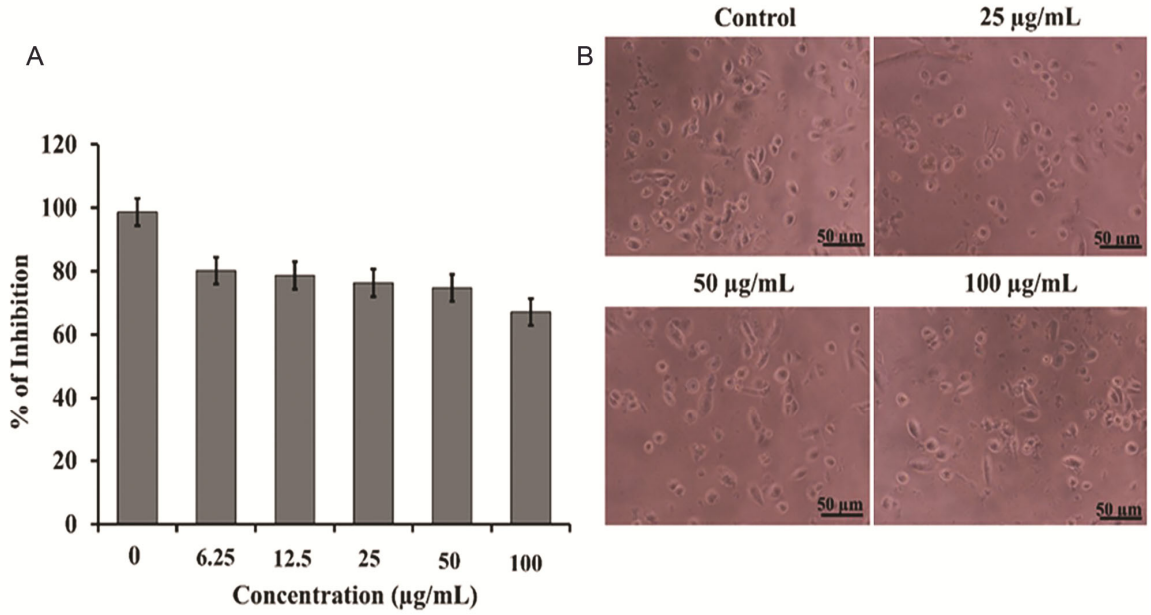

Fig. 3 — Cell death analysis of non-medicated and medicated formula treated HSF cells. MTT assay showing: (A) Cell viability and (B) Morphological changes of treated cells at various concentrations. after 24 h of treatment with *A. judaica* extract. Images were acquired using an inverted microscope (LABOMED®) at 20× magnification.

damage and loss of texture (Fig. 2B). Conversely, no detectable changes in HSF cells treated with ArJ for 24 h, and cells retained their normal spindle-shaped architecture (Fig. 3B). In the BC cells MDA-MB-231, treatment with DOX induced morphological effects at much lower concentrations (Fig. 4B), whereas ArJ induced dose-dependent morphological alterations after 48 hours. At 25 µg/mL, cells began to lose their tumorigenic appearance. At 50 µg/mL, pronounced morphological changes including cell shrinkage, membrane disruption, and reduced adherence—became evident. Treatment with 100 µg/mL caused extensive loss of cell viability and increased detachment in the BC cells MCF-7 (Fig. 5B), T47D (Fig. 6B), and MDA-MB-231 (Fig. 7B). Notably, MDA-MB-231 cells exhibited the most substantial changes after 72 hours exposure to ArJ, supporting the extract′s cytotoxic and pro-apoptotic effects (Fig. 8B).

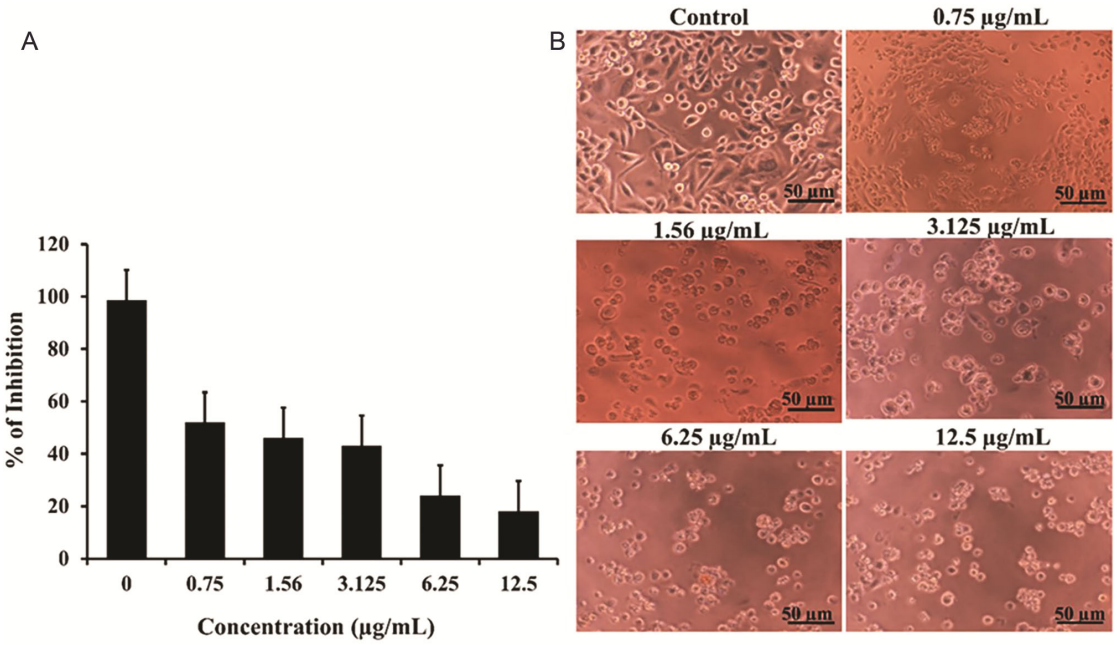

Fig. 4 — Cell death analysis of DOX-treated MDA-MB-231 cells. MTT assay showing: (A) Cell viability after 24 h of treatment and (B) Morphological changes at various concentrations. Images were acquired using an inverted microscope (LABOMED®) at 20× magnification.

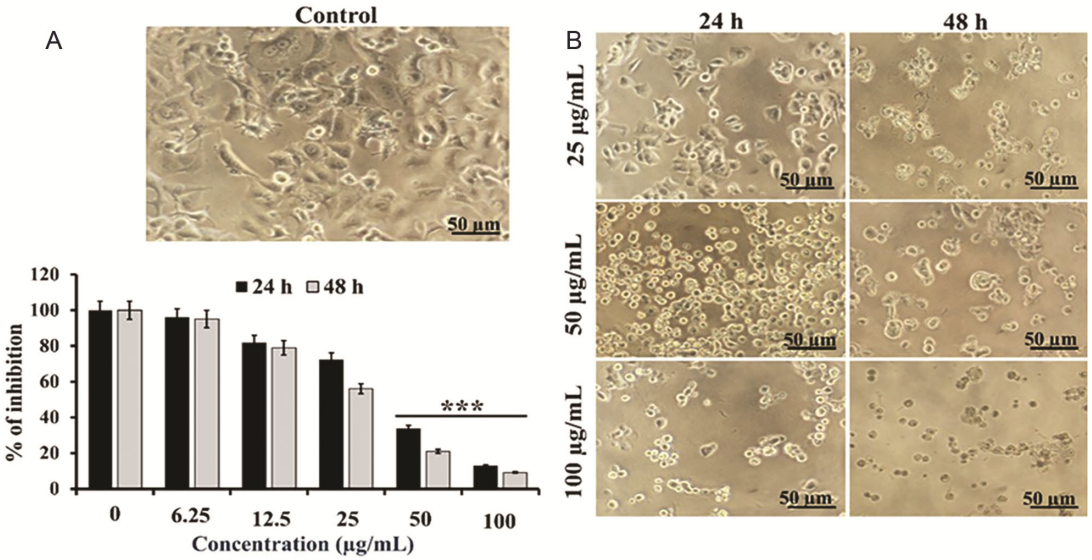

Fig. 5 — Cell death analysis of *A. judaica* extract-treated MCF-7 cells. MTT assay showing: (A) Cell viability after 24 h and 48 h of treatment and (B) Morphological changes at various concentrations. One-way ANOVA followed by Tukey's post hoc test was used to compare treatment groups, with statistical significance set at $P< 0.05$ versus control. Statistical significance at $P< 0.001$ is indicated by triple asterisks (***). Values are expressed as mean ± SD of three independent experiments. Images were acquired using an inverted microscope (LABOMED®) at 20× magnification.

ROS generation analysis

Flow cytometry of CellROS–stained MDA-MB-231 cells demonstrated that both DOX and ArJ significantly increased intracellular ROS levels.A lower fluorescence intensity percentage of 11.4% was determined in untreated (control) cells (Fig. 9A). In contrast, a higher percentage of 58.4% and 56.8% were detected in cells treated with DOX (Fig. 9B) and ArJ extract (Fig. 9C), suggesting increased ROS levels, subsequently decreasing cell population.

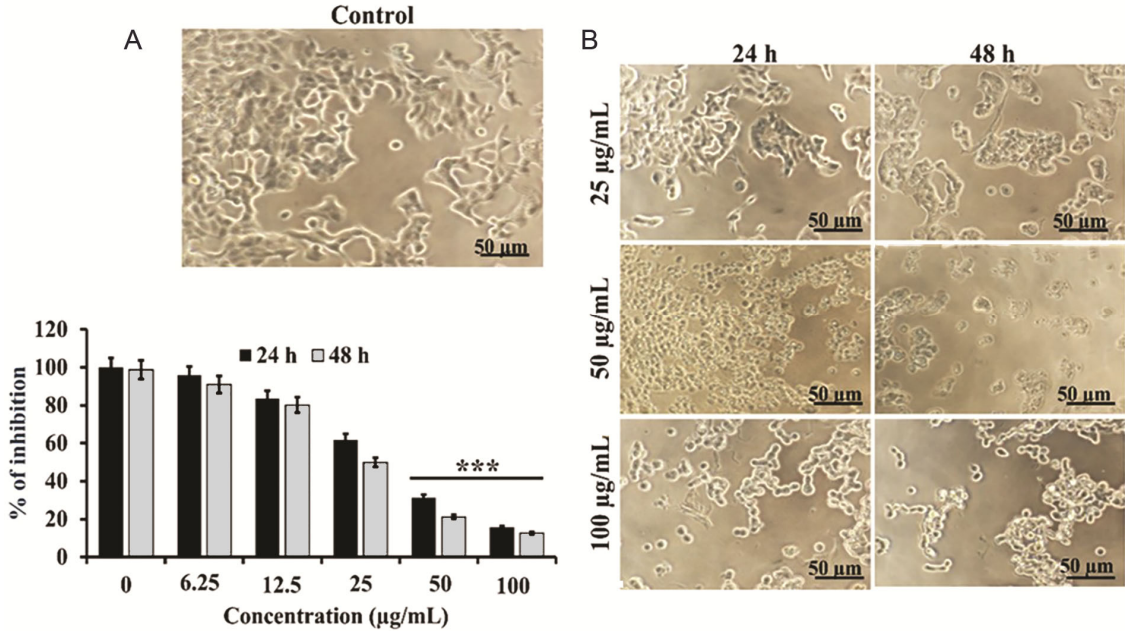

Fig. 6 — Cell death analysis of *A. judaica* extract-treated T47D cells. MTT assay showing: (A) Cell viability after 24 h and 48 h of treatment and (B) Morphological changes at various concentrations. One-way ANOVA followed by Tukey's post hoc test was used to compare treatment groups, with statistical significance set at $P< 0.05$ versus control. Statistical significance at $P< 0.001$ is indicated by triple asterisks (***). Values are expressed as mean ± SD of three independent experiments. Images were acquired using an inverted microscope (LABOMED®, USA) at 20× magnification.

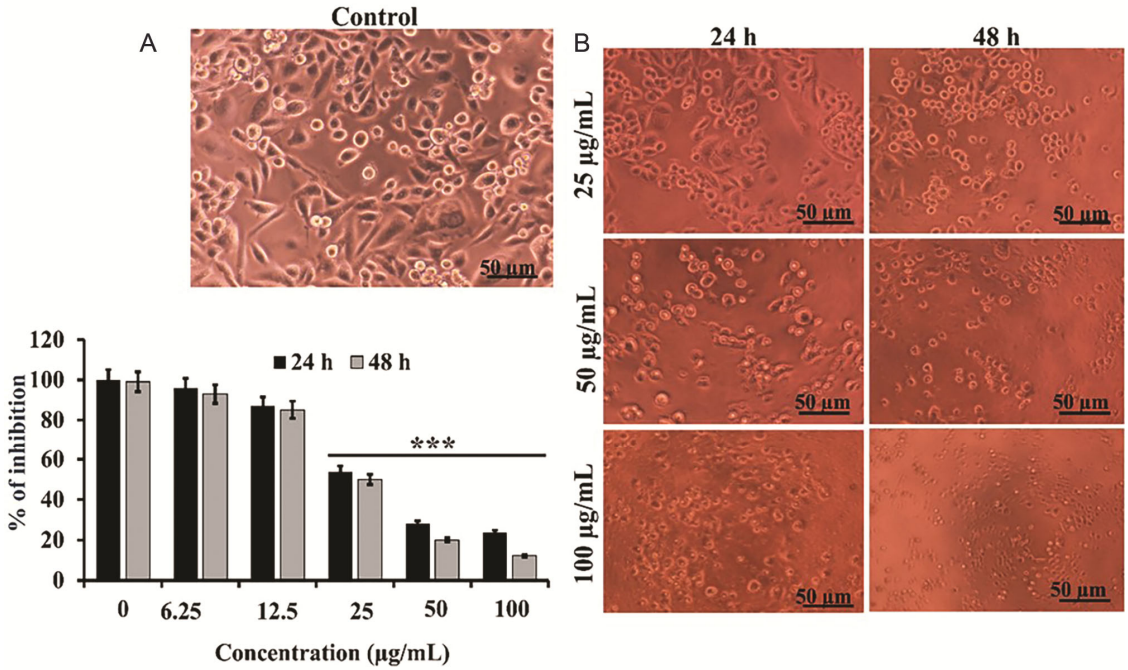

Fig. 7 — Cell death analysis of *A. judaica* extract-treated MDA-MB-231 cells. MTT assay showing: (A)Cell viability after 24 h and 48 h of treatment and (B) Morphological changes at various concentrations. One-way ANOVA followed by Tukey's post hoc test was used to compare treatment groups, with statistical significance set at $P< 0.05$ versus control. Statistical significance at $P< 0.001$ is indicated by triple asterisks (***). Values are expressed as mean ± SD of three independent experiments Images were acquired using an inverted microscope (LABOMED®) at 20× magnification.

Table 3 — IC_{50} values of experimental normal and cancer cell lines treated with DOX and the extracted *A. judaica* L. compounds

			Experimental cell lines		
		HSF	MCF-7	T47D	MDA-MB-231
DOX	24 h	1.135±0.35			1.27±0.12
	24 h	123.9± 3.86	78.22±3.32	98.7±3.88	35.62±2.29
A. judaica L.	48 h		65.07±2.23	77.43±3.22	16.93±2.17
	72 h				9.76±2.03

Table 4 —SI values of ethanolic *A. judaica* L. extracted compounds calculated from experimental cancer cell lines

SI values		Experimental cell lines			Recommended range [1.96-51.3][21]
		MCF-7	T47D	MDA-MB-231	
	24 h	1.58	1.25	3.48	
	48 h	1.90	1.60	7.31	

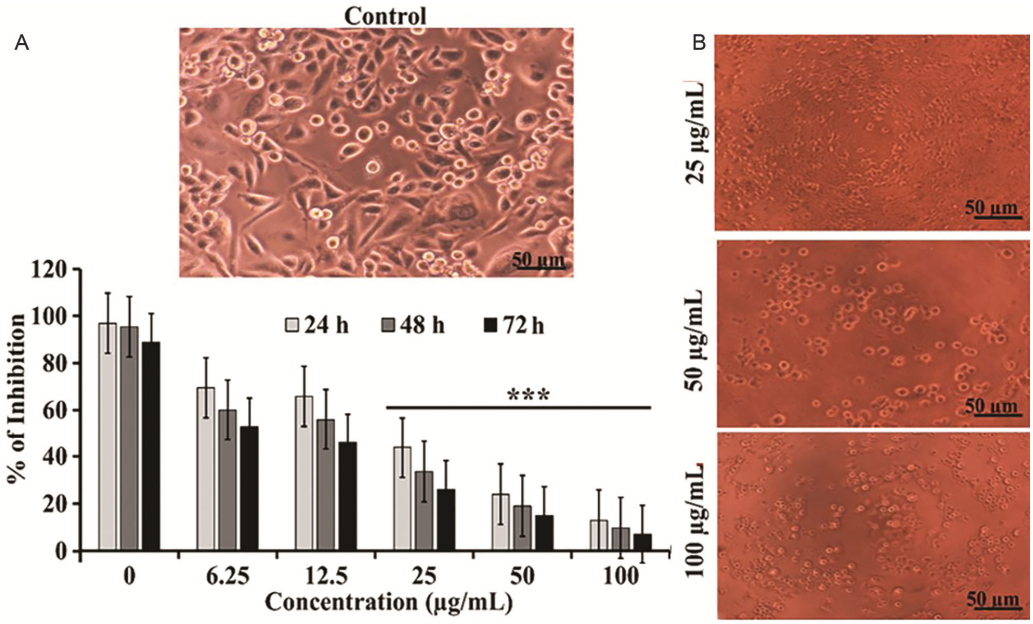

Fig. 8 — Cell death analysis of *A. judaica* extract-treated MDA-MB-231 cells. MTT assay showing: (A) Cell viability after 72 h of treatment and (B) Morphological changes at various concentrations. One-way ANOVA followed by Tukey's post hoc test was used to compare treatment groups, with statistical significance set at $P< 0.05$ versus control. Statistical significance at $P< 0.001$ is indicated by triple asterisks (***). Values are expressed as mean ± SD of three independent experiments. Images were acquired using an inverted microscope (LABOMED®) at 20× magnification.

MMP Disruption analysis

JC-1 staining revealed a marked reduction in MMP following treatment with either DOX or ArJ. The proportion of cells exhibiting intact blue-fluorescent JC-1 aggregates fell to 3.6% (DOX) and 8.2% (ArJ), compared with 88.7% in untreated controls (Fig. 10A- C). The decreased blue fluorescence confirmed mitochondrial depolarization.

Caspase-3 activity

Caspase-3 activity increased in a dose-dependent manner in MDA-MB-231 cells treated with either ArJ or DOX. The Caspase-Glo assay showed a highly significant elevation ($P< 0.001$) in enzyme activity relative to untreated cells (Fig. 11). This supports the involvement of the intrinsic caspase-dependent apoptotic pathway in ArJ-induced cell death.

Cell cycle analysis

Cell cycle profiling revealed that DOX treatment substantially increased the sub-G0 population from 22.7% to 68.7%, with corresponding reductions in G0/G1, S, and G2/M phases. ArJ treatment also increased the sub-G0 population, though to a lesser extent (22.7% to 46.5%). The G0/G1, S, and G2/M phases decreased accordingly (Fig. 12A-C). These

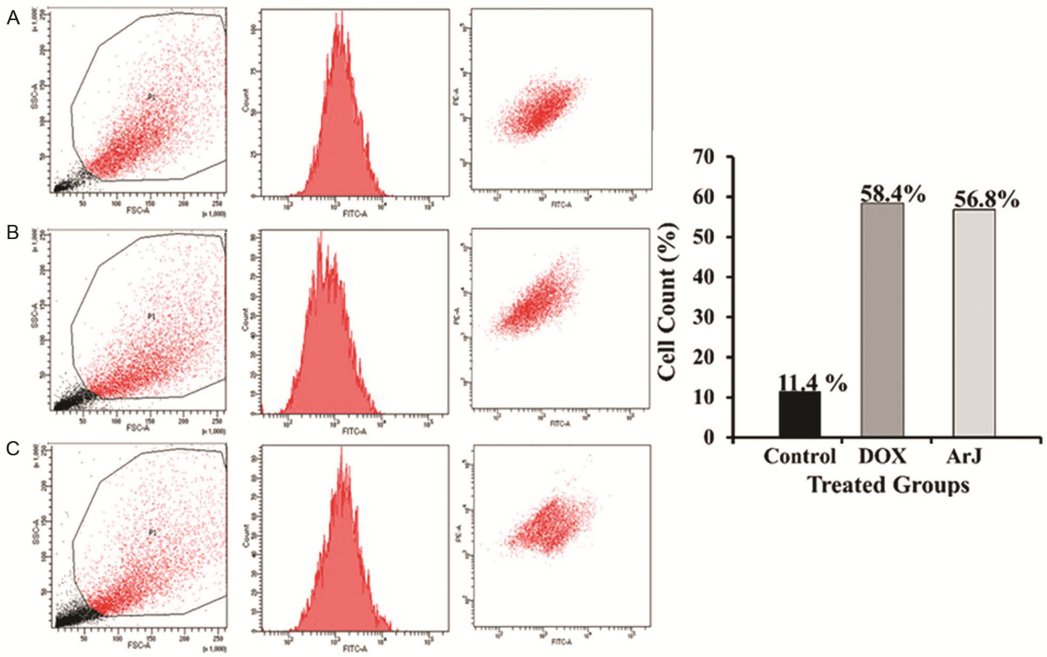

Fig. 9 — The generation of ROS was evaluated by flow cytometry using CellROS in the breast cancer cell line MDA-MB-231: (A) Untreated (control) cells, treated with (B) DOX (2 µg/ml), and (C) ArJ extract (30 µg/ml) for 24 h.

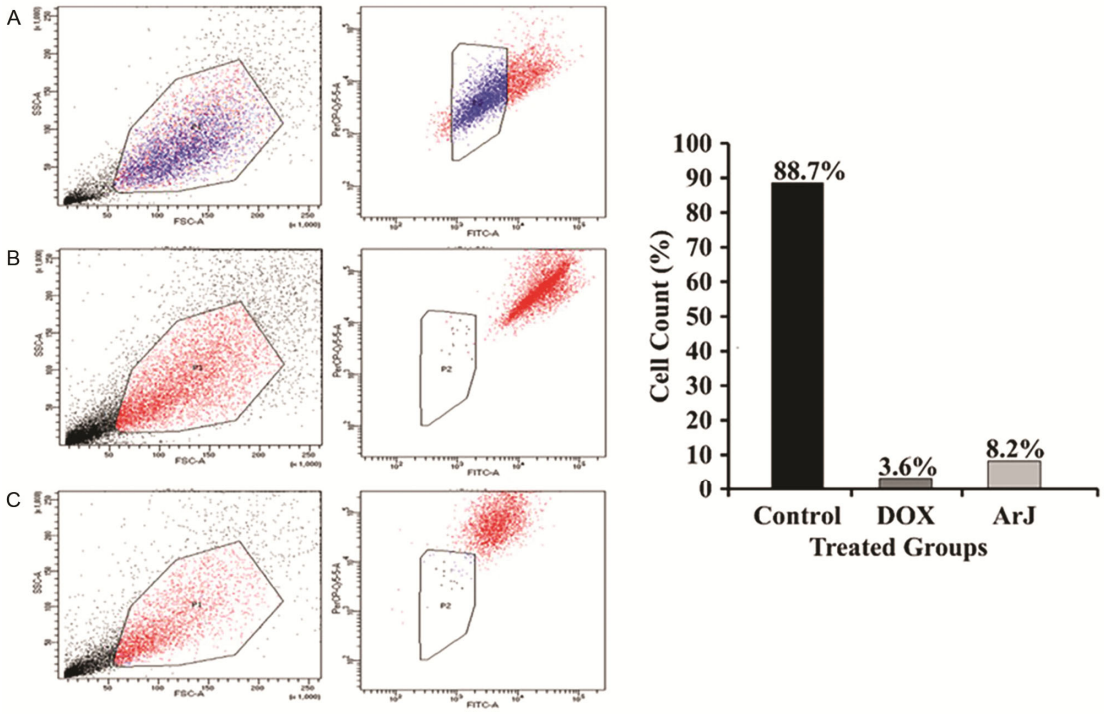

Fig. 10 — Measurement of mitochondrial membrane potential using JC-1 in the breast cancer cell line MDA-MB-231: (A) Untreated (control) cells, treated cells with (B) DOX (2 µg/mL), and (C) ArJ extract (30 µg/mL) for 24 h.

results indicate that ArJ induces apoptosis partly through sub-G0 phase arrest, suggesting cell cycle–dependent cytotoxicity.

Apoptosis detection

Annexin V-FITC/PI staining confirmed that ArJ induces apoptosis in MDA-MB-231 cells. In untreated

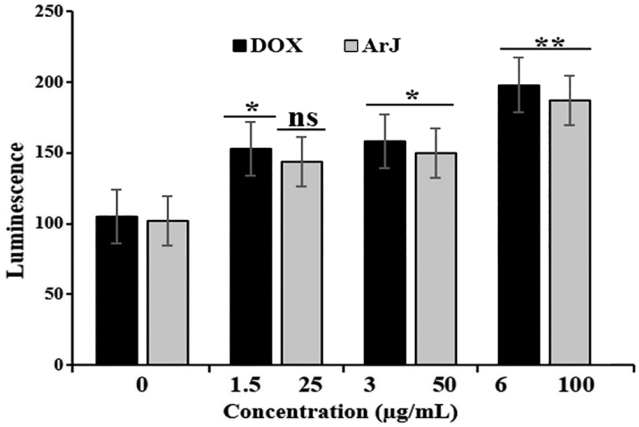

Fig. 11 — Caspase-3 activity was measured after 4 h of treatment with DOX and ArJ extract at different concentrations in the breast cancer cell line MDA-MB-231 using luminescence by a microplate reader. A significant increase was observed in the activity of both the caspases treated with DOX and ArJ. *P*-value < 0.05 was considered significant (*). *P*-value < 0.001 was represented by an asterisk (**).

controls, 88.6% of cells were viable. In contrast, viability decreased to 6.1% with DOX and 2.2% with ArJ after 24 hours. Early apoptotic populations increased slightly (1.87% for DOX; 0.7% for ArJ), while late apoptosis increased markedly (38% for DOX; 96% for ArJ) (Fig. 13A-C). These findings demonstrate that ArJ predominantly induces late-stage apoptosis with minimal necrosis.

Discussion

Globally, BC remains the most frequently diagnosed malignancy among women, and its incidence has continued to rise over the past decades. In 2020, more than 2 million new BC cases and over 500,000 related deaths were reported, and projections estimate that global incidence will exceed 3 million new cases with nearly 1 million annual deaths by 2040 due to population growth and aging populations[26]. Among BC subtypes, TNBC is

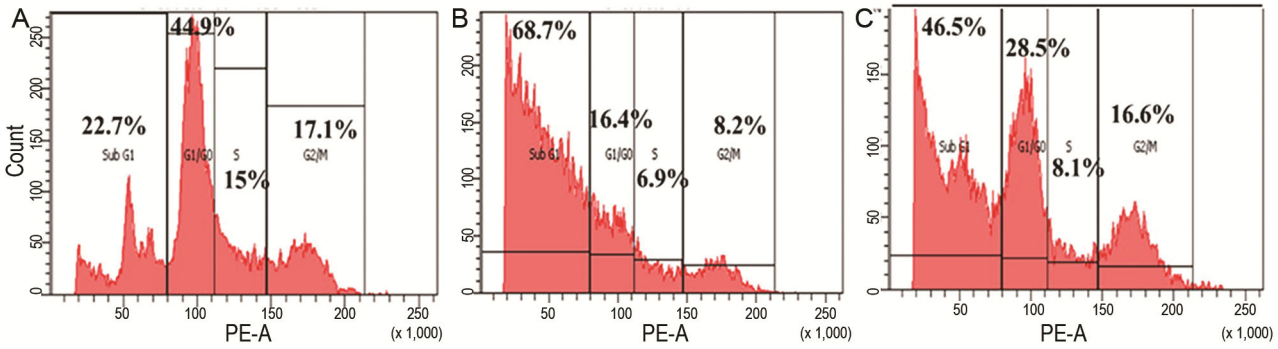

Fig. 12 — Flow cytometric analysis of cell cycle arrest in breast cancer cell line MDA-MB-231 showing cell population percentages of cell cycle phases: (A) Untreated (control) cells, treated cells with (B) DOX (2 µg/mL), and (C) ArJ extract (30 µg/mL) for 24 h.

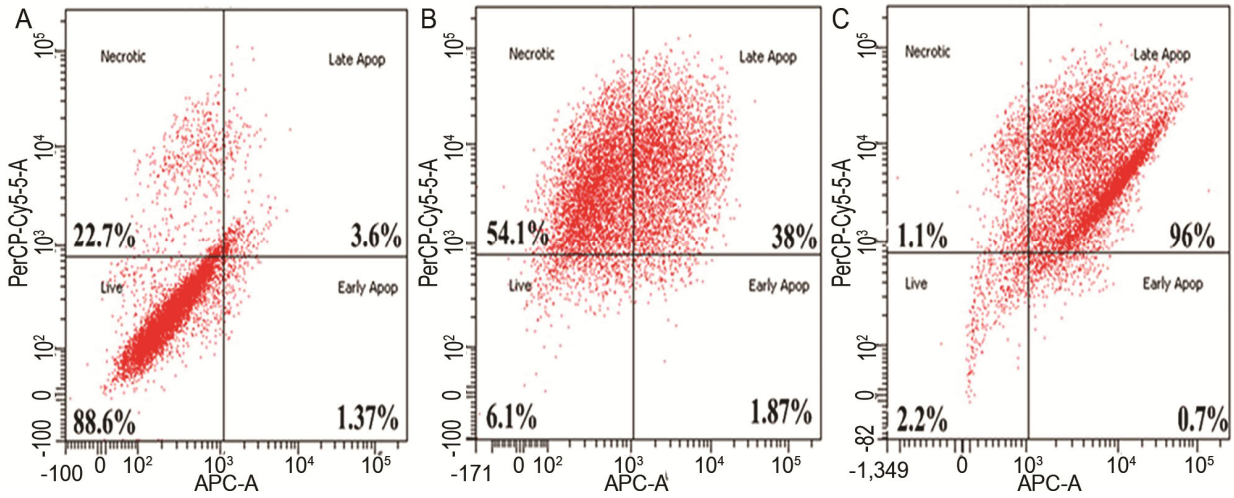

Fig. 13 — Detection of apoptosis was evaluated using annexin V-FITC in the breast cancer cell line MDA-MB-231 showing cell population distributions in different apoptotic phases: (A) Untreated (control) cells, treated cells with (B) DOX (2 µg/mL), and (C) ArJ extract (30 µg/mL) for 24 h.

associated with the poorest clinical outcomes because of its molecular heterogeneity, lack of hormone receptors, and intrinsic resistance to conventional therapies. These challenges underscore the need for alternative treatment strategies and the exploration of natural compounds with selective anticancer properties.

Biochemical characterisation using spectroscopic and spectrometric techniques is increasingly employed to identify and quantify bioactive constituents in medicinal plants. Such analytical approaches provide precise functional group identification and support the discovery of pharmacologically active molecules[27]. In this study, we analysed the chemical composition of the ethanolic extract of ArJ. Ethanol was selected as the extraction solvent because it is a safe, polar, and highly efficient solvent capable of extracting both hydrophilic and moderately lipophilic phytochemicals, particularly phenolics and flavonoids[28].

FTIR spectroscopy of ArJ extract revealed characteristic peaks corresponding to phenolic O–H groups (2.93), aromatic amines (2.02) and ester C=O functionalities (1.77). These findings highlight the richness of phenolic and aromatic constituents known for their antioxidant, anti-inflammatory, and antiproliferative activities. Complementary GC–MS analysis identified multiple heterocyclic aromatic compounds exhibiting documented anticancer potential. Benzamide derivatives are known histone deacetylase (HDAC) inhibitors that promote chromatin condensation, induce cell-cycle arrest, and trigger apoptosis in breast cancer cells[29]. Oxadiazine compounds exhibit strong antiproliferative effects through mitochondrial membrane disruption[30]. Benzofuran-carboxylic acids can influence the hypoxic tumor microenvironment by modulating the HIF-1α/VEGF axis[31], while pyrimidine-based molecules have been shown to suppress TNBC invasion and proliferation through FAK-mediated signaling[32]. These reported mechanisms support the hypothesis that the aromatics identified in ArJ contribute to its cytotoxic activity.

DOX was used as a positive control because it remains one of the most effective chemotherapeutic agents for BC[33], despite its well-known drawbacks, including cardiotoxicity and acquired drug resistance. SI evaluation demonstrated that unlike DOX, the ArJ extract showed favourable selectivity toward cancer cells, with minimal toxicity toward normal HSF cells. This observation aligns with previous studies reporting low toxicity of *Artemisia* extracts in normal cell lines[34]. Morphological alterations including cell shrinkage, chromatin condensation, and detachment further confirmed the antiproliferative and pro-apoptotic effects of ArJ at concentrations lower than those required for DOX-induced cytotoxicity.

Natural products continue to play a central role in anticancer drug discovery[35]. Consistent with earlier reports, our results show that ArJ extract demonstrated the highest cytotoxicity against the metastatic MDA-MB-231 TNBC cells, followed by moderate effects on MCF-7 and T47D cells[36,37]. This differential sensitivity may be attributed to the higher metabolic and oxidative vulnerability of TNBC cells.

ROS are key regulators of cancer cell survival, genomic instability, and metastasis[38,39]. Modulating ROS levels is an established strategy for inducing cancer-selective apoptosis. In this study, ArJ extract significantly increased intracellular ROS in MDA-MB-231 cells, comparable to or exceeding the levels induced by DOX. This elevated ROS production likely results from interactions between ArJ antioxidant molecules and cellular free radicals, leading to oxidative imbalance[40]. Similar ROS-elevating effects have been documented in *Artemisia* species from Saudi Arabia[41].

MMP disruption is a hallmark of intrinsic apoptosis. JC-1 staining confirmed substantial mitochondrial depolarization following ArJ treatment, consistent with ROS accumulation, mitochondrial membrane rupture, and cytochrome-c release. These findings parallel those observed with cirsimaritin, a dominant flavone in *A. judaica*, which also promotes apoptosis through ROS-mediated mitochondrial damage[42].

Apoptosis execution requires activation of effector caspases, especially caspase-3[43]. ArJ extract significantly elevated caspase-3 activity in MDA-MB-231 cells, supporting activation of the intrinsic apoptotic pathway, as previously reported for other *Artemisia* extracts[44]. Additionally, cell cycle analysis showed accumulation of cells in the sub-G1 phase, indicating DNA fragmentation, while Annexin V/PI staining confirmed predominant late apoptosis with minimal necrosis. These results are consistent with earlier studies demonstrating that *Artemisia* species induce mitochondrial-dependent apoptosis in cancer cells[45].

Collectively, our findings indicate that *Artemisia judaica* ethanolic extract exerts selective and potent

cytotoxic effects on MDA-MB-231 cells through a ROS-mediated mitochondrial pathway involving MMP loss, caspase-3 activation, and cell cycle arrest. The presence of multiple bioactive heterocyclic and aromatic compounds further underscores the therapeutic potential of this plant. Future investigations should focus on isolating individual compounds, validating molecular targets, and conducting *in vivo* studies to advance ArJ-derived molecules toward preclinical and clinical development.

Conclusion

The ethanolic extract of ArJ leaves was found to contain phenyl-amino-benzoic acid derivatives and other bioactive heterocyclic compounds with notable anticancer potential. These constituents exhibited selective cytotoxicity toward breast cancer cells, particularly the highly aggressive triple-TNBC subtype while maintaining minimal toxicity toward normal cells. Mechanistic analyses revealed that ArJ extract suppresses cancer cell proliferation by inducing oxidative stress, disrupting mitochondrial membrane potential, and activating the intrinsic apoptotic pathway through caspase-3 signaling. Additionally, ArJ treatment caused cell cycle arrest at the sub-G1 and G0/G1 phases and significantly increased the proportion of late apoptotic cells, as confirmed by Annexin V/PI staining, with negligible necrosis. Chemical profiling using FTIR and GC–MS identified key phytochemicals, including phenolics, aromatic amines, esters, benzamide derivatives, oxadiazines, and benzofuran-carboxylic acids. These compounds may underlie the observed anticancer activity and could contribute to modulation of signaling pathways involved in cell proliferation, migration, and invasion in aggressive metastatic TNBC cells. Overall, the findings indicate that ArJ-derived compounds hold promise as natural anticancer agents with selective activity and lower toxicity compared with conventional chemotherapeutics. Further in-depth preclinical studies, followed by clinical evaluation, are required to validate their therapeutic potential and support the development of ArJ-based treatments for aggressive breast cancer subtypes, particularly MDA-MB-231 cells.

Acknowledgment

The Deanship of Scientific Research (DSR) at King Abdulaziz University (KAU), Jeddah, Saudi Arabia has funded this Project under grant no (G: 653-130-1443).

Conflict of interest

The authors declare no conflict of interest.

References

1 Sung H, Ferlay J, Siegel RL, Laversanne M, Soerjomataram I, Jemal A & Bray F. Global cancer statistics 2020: GLOBOCAN estimates of incidence and mortality worldwide for 36 cancers in 185 countries. *CA Cancer J Clin*, 71 (2021) 209.

2 Bray F, Laversanne M, Weiderpass E & Soerjomataram I. The ever-increasing importance of cancer as a leading cause of premature death worldwide. *Cancer*, 127 (2021) 3029.

3 Orrantia-Borunda E, Anchondo-Nuñez P, Acuña-Aguilar E, Gómez-Valles O & Ramírez-Valdespino A. Subtypes of breast cancer. *Breast Cancer*, 2022.

4 Zagami P & Carey A. Triple negative breast cancer: Pitfalls and progress. *NPJ Breast Cancer*, 8 (2022) 95.

5 Bergin ART & Loi S. Triple-negative breast cancer: recent treatment advances. *F1000Res*, 8 (2019) 1342.

6 Mamatova AS, Korona-Glowniak I, Skalicka-Woźniak K, Józefczy A, Wojtanowski KK, Baj T, Sakipova ZB & Malm A. Phytochemical composition of wormwood (Artemisia gmelinii) extracts in respect of their antimicrobial activity. *BMC Complement Altern Med*, 19 (2019) 288.

7 El-Nashar A, Eldahshan A, Nilofar N & Zengin G. Chemical profiling and enzyme inhibitory properties of essential oil isolated from Artemisia judaica grown in Egypt: GC-MS analysis and in-vitro studies. *Natural Product Research*, 1 (2024) 5.

8 Khan M, Khan M, Al-Hamoud K, Adil SF, Shaik MR & Alkhathlan HZ. Comprehensive phytochemical analysis of various solvent extracts of Artemisia judaica and their potential anticancer and antimicrobial activities. *Life (Basel)*, 12 (2022) 1885.

9 Bisht D, Kumar D, Kumar D, Dua K & Chellappan DK. Phytochemistry and pharmacological activity of the genus Artemisia. *Arch Pharm Res*, 44 (2021) 439.

10 Peng Y, Felce SL, Dong D, Penkava F, Mentzer AJ, Yao X. An immunodominant NP105-113-B*07:02 cytotoxic T cell response controls viral replication and is associated with less severe COVID-19 disease. *Nat Immunol*, 23 (2022) 50.

11 Pezuk JA. Pyroptosis in combinatorial treatment to improve cancer patients' outcome, is that what we want? *EBioMedicine*, 41 (2019) 17.

12 Li J, Cao F, Yin HL, Huang ZJ, Lin ZT, Mao N, Sun B & Wang G. Ferroptosis: past, present and future. *Cell Death Dis*, 11 (2020) 88.

13 Greco G, Catanzaro E & Fimognari C. Natural products as inducers of non-canonical cell death: a weapon against cancer. *Cancers (Basel)*, 13 (2021) 304.

14 Feng S, Zha Z, Wang Z, Yang P, Wu J, Li X & Liu Y. Anticancer activity of oleiferoside B involving autophagy and apoptosis through increasing ROS release in MCF-7 and SMMC-7721 cells. *Nat Prod Res*, 35 (2021) 4865.

15 Singh R, Letai A & Sarosiek K. Regulation of apoptosis in health and disease: the balancing act of BCL-2 family proteins. *Nat Rev Mol Cell Biol*, 20 (2019) 175.

16 Carneiro A & El-Deiry S. Targeting apoptosis in cancer therapy. *Nat Rev Clin Oncol*, 17 (2020) 395.

17 Shahmoradi R, Talebibahmanbigloo N, Javidparvar A, Bahlakeh M & Ramezanzadeh B. Studying the

adsorption/inhibition impact of cellulose and lignin compounds extracted from agricultural waste on mild steel corrosion in HCl solution. *J Mol Liquids*, 304 (2020) 112751.
18 Pangesti P & Masruri M. Consistency of spectra and antibacterial activity of extract mixture of Curcuma longa, Zingiber officinale, and Syzygium aromaticum. *IOP Conf Ser Mater Sci Eng*, 833 (2020) 012033.
19 Hago S, Lu T, Alzain A, Abdelgadir A, Yassin S, Ahmed M & Xu H. Phytochemical constituents, in-vitro anticancer activity and computational studies of Cymbopogon schoenanthus. *Natural Product Research*, 38 (2024) 1073.
20 Kamiloglu S, Sari G, Ozdal T & Capanoglu E. Guidelines for cell viability assays. *Food Frontiers*, 1 (2020) 332.
21 Indrayanto G, Putra GS & Suhud F. Validation of in-vitro bioassay methods: application in herbal drug research. *Profiles Drug Subst Excip Relat Methodol*, 46 (2021) 273.
22 Qi LF, Xu ZR, Li Y, Jiang X & Han XY. In vitro effects of chitosan nanoparticles on proliferation of human gastric carcinoma MGC803 cells. *World J Gastroenterol*, 11 (2005) 5136.
23 Wang HQ, Sun XB, Xu YX, Zhao H, Zhu QY & Zhu CQ. Astaxanthin upregulates heme oxygenase-1 expression through ERK1/2 pathway and protects against β-amyloid cytotoxicity in SH-SY5Y cells. *Brain Res*, 1360 (2010) 159.
24 Fried J, Perez AG & Clarkson BD. Flow cytofluorometric analysis of cell cycle distributions using propidium iodide. *J Cell Biol*, 71 (1976) 172.
25 Kumar R, Saneja A & Panda AK. An annexin V-FITC/propidium iodide-based method for detecting apoptosis in non-small cell lung cancer. *Lung Cancer: Methods and Protocols*, 213 (2021) 223.
26 Arnold M, Morgan E, Rumgay H, Mafra A, Singh D, Laversanne M, Vignat J, Gralow JR, Cardoso F, Siesling S, Soerjomataram I. Current and future burden of breast cancer: Global statistics for 2020 and 2040. *Breast*, 66 (2022) 15.
27 Lozada-Ramírez D, Ortega-Regules E, Hernández & Anaya de Parrodi C. Spectroscopic and spectrometric applications for identifying bioactive compounds from vegetal extracts. *Appl Sci*, 11 (2021) 3039.
28 Abubakar AR & Haque M. Preparation of medicinal plants: basic extraction and fractionation procedures for experimental purposes. *J Pharm Bioallied Sci*, 12 (2020) 1.
29 Movafagh S & Munson A. Histone deacetylase inhibitors in cancer prevention and therapy. *Epigenetics of Cancer Prevention*, 75 (2019) 105.
30 Sousa ML, Preto M, Vasconcelos V, Linder S & Urbatzka R. Antiproliferative effects of the natural oxadiazine nocuolin A are associated with impaired mitochondrial oxidative phosphorylation. *Front Oncol*, 9 (2019) 224.
31 Eldehna WM, Nocentini A, Elsayed ZM, Al-Warhi T, Aljaeed N, Alotaibi OJ, Al-Sanea MM, Abdel-Aziz HA & Supuran CT. Benzofuran-based carboxylic acids as carbonic anhydrase inhibitors and antiproliferative agents against breast cancer. *ACS Med Chem Lett*, 11 (2020) 1022.
32 Zhang J, Xu K, Yang F, Qiu Y, Li J, Li J, Wang W, Tan G, Zou Z & Kang F. Nitric oxide-releasing derivatives of 2, 4-diaminopyrimidine as novel FAK inhibitors for metastatic triple-negative breast cancer. *Eur J Med Chem*, 250 (2023) 115192.
33 Christowitz C, Davis T, Isaacs A, van Niekerk G, Hattingh S & Engelbrecht AM. Mechanisms of doxorubicin-induced drug resistance and tumour growth in a murine breast tumour model. *BMC Cancer*, 19 (2019) 757.
34 Qanash H, Bazaid AS, Aldarhami A, Alharb B, Almashjary MN, Hazzazi MS, Felemban HR & Abdelghany TM. Phytochemical characterization and efficacy of Artemisia judaica extract-loaded chitosan nanoparticles. *Polymers (Basel)*, 15 (2023) 391.
35 Atanasov AG, Zotchev SB, Dirsc VM, International Natural Product Sciences Taskforce & Supuran, CT. Natural products in drug discovery: advances and opportunities. *Nat Rev Drug Discov*, 20 (2021) 200.
36 Goda S, Nafie S, Awad M, Abdel-Kader S, Ibrahim K, Badr M & Eltamany E. *In vitro* and *in vivo* anti-lung cancer activity of Artemisia judaica L. with LC-MS/MS profiling and docking studies. *Antioxidants*, 11 (2021) 17.
37 Nasr A, Noman M, Mothana A, Alqahtani S & Al-Mishari A. Cytotoxic, antimicrobial and antioxidant activities of Artemisia judaica and A. sieberi in Saudi Arabia. *Afr J Pharm Pharmacol*, 14 (2020) 278.
38 Fuloria S, Subramaniyan V, Karupiah S, Kumari U, Sathasivam K, Meenakshi DU, Wu YS, Guad RM, Udupa K & Fuloria NK. Reactive carbonyl species in chronic diseases: source, effects, detection and management. *Antioxidants (Basel)*, 9 (2020) 1075.
39 Sarmiento-Salinas FL, Perez-Gonzalez A, Acosta-Casique A, Ix-Ballote A, Diaz A, Treviño S, Rosas-Murrieta NH, Millán-Perez-Peña L & Maycotte P. Reactive oxygen species in carcinogenesis and tumor progression. *Life Sci*, 284 (2021) 119942.
40 Firczuk M, Bajor M, Graczyk-Jarzynka A, Fidyt, K, Goral A & Zagozdzon R. Harnessing altered oxidative metabolism in cancer by augmented pro-oxidant therapy. *Cancer Lett*, 471 (2020) 1.
41 Salih AM, Qahtan AA & Al-Qurainy F. Phytochemical identification and bioactive compound estimation of Artemisia species grown in Saudi Arabia. *Metabolites*, 13 (2023) 443.
42 Benali T, Jaouadi I, Ghchime R, El Omari N, Harboul K, Hammani K, Rebezov M. Current knowledge on biological properties of cirsimaritin. *Antioxidants (Basel)*, 11 (2022) 1842.
43 Cui J, Zhao S, Li Y, Zhang D, Wang B, Xie J & Wang J. Regulated cell death: discovery, features and implications for neurodegenerative diseases. *Cell Commun Signal*, 19 (2021) 29.
44 Younes M, Bin K, Unissa R, Almarshdi A, Alharbi M, Alenzi S & Abouzied S. Anti-microbial and cytotoxic activity of Artemisia judaica leaves and stems via caspase-dependent apoptosis. *Indian J Pharm Educ Res*, 56 (2022) s52.
45 Kamarya Y, Lijie X & Jinyao L. Chemical constituents and antitumor mechanisms of Artemisia. *Anticancer Agents Med Chem*, 22 (2022) 1838.